PHILOSOPHICAL TRANSACTIONS OF THE ROYAL SOCIETY A MATHEMATICAL, PHYSICAL & ENGINEERING SCIENCES

NMR Microscopy of the Germinating Castor Bean

P. G. Morris, H. E. Darceuil, A. Jasinski, A. K. Jha, D. J. O. McIntyre and D. H. Northcote

Phil. Trans. R. Soc. Lond. A 1990 **333**, 487-493
doi: 10.1098/rsta.1990.0176

NMR microscopy of the germinating castor bean

By P. G. Morris[1], H. E. Darceuil[1], A. Jasinski[2], A. K. Jha[1], D. J. O. McIntyre[1] and D. H. Northcote[1]

[1] *Department of Biochemistry, University of Cambridge, Tennis Court Road, Cambridge CB2 1QW, U.K.*

[2] *Institute of Nuclear Physics, ul. Radzikowskiego 152, 31-342 Krakow, Poland*

Water uptake is the trigger for germination and growth. It is a triphasic process, involving a rapid rehydration of the endosperm, a steady uptake during a period of active metabolism and finally, a rapid uptake during development of the root system. The water spin lattice relaxation time (T_1) of the germinating seed of the castor bean (*Ricinus communis zanzibariensis*) apparently decreases with increasing water content. This anomalous behaviour is resolved when the recovery process is analysed as two components: each component shows the expected dependence on water content but the proportion of the faster relaxing component increases during development. NMR microscopy is used to investigate the location of these water compartments and to follow the anatomical changes which occur during the germination and early growth processes.

1. Introduction

Germination is the process during which the stored energy reserves within a seed (polysaccharide, protein and lipid) are mobilized and new materials are synthesized for growth and development. This dramatic initiation of rapid metabolic activity culminates in the growth and protrusion of the embryo from the seed coat that may be thought of as the end of successful germination. During the subsequent early growth phase, the embryo continues to develop into a seedling. Water plays the primary role both in the initiation and in the perpetuation of these vital processes.

Quiescent seeds of higher plants are essentially dehydrated; their water content may drop to about 10% of the total weight compared with in excess of 70% in developing plant tissues. The reuptake of water by seeds is a triphasic process (see, for example, Bewley & Black 1978). Germination is initiated by a rapid uptake of water in phase I, a process lasting some 24 h and known as imbibition. It is primarily the protein, which in the case of the castor bean (*Ricinus communis zanzibariensis*) accounts for about 18% of the dry weight of the seed, that imbibes the water. Imbibition occurs in all seeds, alive or dead. In viable seeds, it triggers the rapid metabolic activity required to mobilize food reserves to supply the needs of the developing embryo. Water uptake is less dramatic, but is sustained over the whole of this phase II process which, in *R. communis*, lasts typically 4–5 days. During phase III, the seed germinates and the seedling develops rapidly. The rate of water uptake again rises steeply.

Much is known of the chain of biochemical events leading to germination in *R. communis* (Marriot & Northcote 1975*a*, *b*; Martin & Northcote 1981). However, it has not so far been possible to study the primary event, water uptake, at the

microscopic level. It is of particular interest to follow the differential uptake of water by the anatomically distinct regions of the seed. It is all the more interesting if the state (free or bound) of the water can be simultaneously monitored. The developing technique of NMR microscopy (see, for example, Morris *et al.* 1990) offers us a unique window into this crucial process. The main attraction of an NMR imaging technique in this work is the direct observation of the substance of interest, namely, water. Furthermore, the NMR relaxation properties of the water protons reflect its state; the level of hydration, what fraction is bound to macromolecules and how tightly. Because the technique is non-destructive, it is possible to perform these measurements in serial fashion over several days on the same seed. This is important because it permits us to check that the seed is viable (i.e. goes on to germinate and develop into a normal seedling). It also avoids the problems associated with the inherent genetic variability of seeds which make true serial studies impossible using destructive microscopic techniques. A further obvious benefit of NMR microscopy is that it is not a surface technique: slices at any depth and orientation can be selected, or indeed, as in the study reported here, a full three-dimensional image, containing information from all volume elements through the structure can be generated.

2. NMR microscope

The NMR microscope used for the studies described below was developed in the Department of Biochemistry in Cambridge based on a Bruker AM400 widebore (89 mm) spectrometer (Morris *et al.* 1990). To this standard configuration were added a magnetic field gradient controller, gradient coils, microscopy probehead and image display. The gradient controller comprises waveform memories for each of three orthogonal gradient channels (Frenkiel *et al.* 1988). The contents of these memories can be clocked out through fast digital multipliers for a particularly straightforward implementation of the (spin warp) Fourier imaging scheme used for these studies (Edelstein *et al.* 1980). Two gradient coil sets are available: a 'large bore' set, generating gradients of approximately 1 G cm^{-1} A^{-1} and a 'small bore' version, generating gradients of approximately ten times this value. The maximum gradient we can generate using the latter system is approximately 100 G cm^{-1}.

Three-dimensional Fourier imaging sequences are used to generate images with 128, 64 and 32 points in x, y and z-dimensions, respectively. Normally this volume data set is displayed as thirty-two 128×64 slices normal to z. For high-resolution work, a three-turn solenoidal probehead is used with an internal diameter of 3.6 mm. Adjusting the gradient amplitude to give an isotropic resolution of 40 μm, the one-shot (i.e. one free induction decay per gradient increment) signal-to-noise ratio (SNR) from a water-filled capillary is about 150:1. This indicates that the isotropic resolution limit on the microscope as it presently stands is on the order of a few micrometres, for reasonable imaging times. (Higher in-plane resolution can of course be achieved at the same SNR from thicker slices provided the volume corresponding to each pixel remains unchanged.)

For the experiments on castor bean seeds, the same image matrix was used with rather lower resolution to fully cover the castor bean seed. The seeds have high lipid contents at the start of imbibition (60% of the endosperm dry mass). This falls during germination as the food reserves are mobilized and utilized for growth. At the proton NMR frequency of 400 MHz, the chemical shift difference of *ca.* 3.5 p.p.m. between water and methylene protons suggests that it might be possible to generate

PHILOSOPHICAL TRANSACTIONS OF THE ROYAL SOCIETY A MATHEMATICAL, PHYSICAL & ENGINEERING SCIENCES

completely separated water and lipid images. However, the water T_2 relaxation times are sufficiently short as to necessitate large frequency encoding gradients, precluding the use of such a simple device. Suppression of the lipid signal by initial presaturation of the methylene resonance (in the absence of any applied field gradient) was used to generate pure water images. Pure lipid images could be generated by a similar method or by subtraction of the pure water image from an uncorrected image containing both water and (displaced) lipid signals.

To pick out water components with specific spin lattice relaxation time (T_1) values, both partial saturation and inversion null sequences were used. In the former, the repetition time (T_R) of the imaging sequence was varied to favour a particular component. In the latter a component with a particular T_1 value could be eliminated by application of a hard inversion pulse followed by a delay (T_I) sufficient for the component to recover just to zero before the start of the Fourier imaging sequence. Lipid suppression in the form of a presaturation pulse was optionally applied both before and during the T_I recovery delay.

3. Water content and relaxation time measurements

In preliminary images of the germinating castor bean system, the anatomical definition and the SNR were found to be substantially less than expected from tests of the NMR microscope on phantoms. This prompted a detailed study of the NMR relaxation properties of the castor bean during germination. Measurements were made on whole seeds from which the testa had been removed before the start of imbibition (Martin & Northcote 1981). The initial and the final fresh masses, following variable periods of water uptake, were recorded. T_1 and T_2 values were determined by the inversion recovery and Car–Purcell spin echo methods, respectively, using an exponential fitting routine.

The lipid relaxation times were unremarkable. T_1 values were between 440 and 510 ms for the full range of water uptake times (0–100 h), with a very slight tendency towards longer relaxation times at higher water contents. The lipid T_2 values showed a slightly more pronounced variation with water content, increasing from an initial value of 17 ms to a value after 100 h water uptake of 21 ms.

Water T_2 measurements revealed a multiexponential decay with a $T_{\frac{1}{2}}$ of less than 10 ms; typically 3 ms initially, increasing to 9 ms after 100 h water uptake. This was clearly the explanation for the poor quality images obtained in the preliminary studies. Water T_1 measurements brought some surprises, as illustrated in figure 1. It shows measurements as a function of water uptake time (a) and as a function of the proportional increase in the initial fresh mass (b). The apparent decrease in T_1 with water content is the opposite behaviour to that observed in other biological systems (see, for example, Morris 1986). It led us to undertake more detailed analyses. The data shown in figure 1 are derived from measurements made on many different seeds. Genetic variability may well give rise to the considerable scatter in the results. However, it cannot account for the underlying trend. To get tighter data, single seeds were followed through the water uptake timecourse. It was noted that the fit of the relaxation data to a single exponential was less than perfect. Accordingly, the fitting routine was allowed to characterize the magnetization recovery by two exponential curves. A typical result of this analysis is shown in figure 2. The analysis in terms of a two-component system has reassuring features. First, each component has T_1 values which show the expected increase with water content. (The reason for the

PHILOSOPHICAL TRANSACTIONS OF THE ROYAL SOCIETY A MATHEMATICAL, PHYSICAL & ENGINEERING SCIENCES

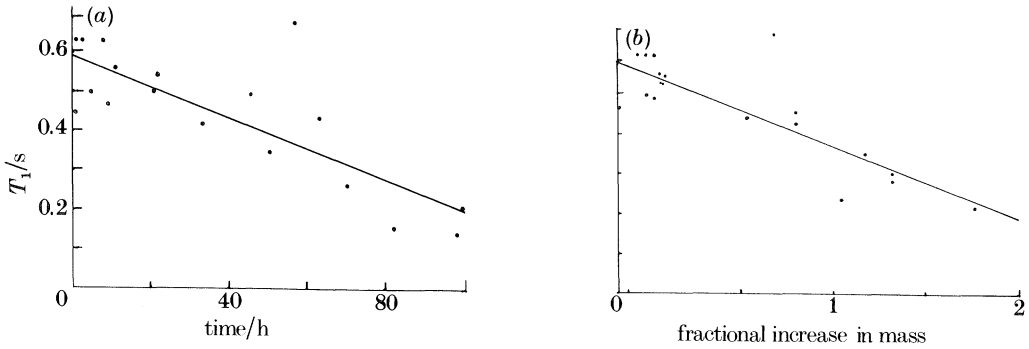

Figure 1. The spin lattice relaxation time, T_1, of water in germinating castor beans as a function of the time of imbibition (*a*) and as a function of the fractional increase in fresh mass (*b*).

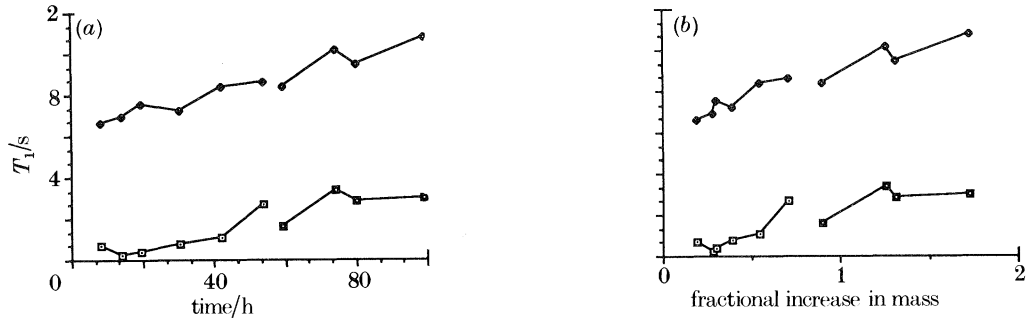

Figure 2. Two component analysis of T_1 relaxation behaviour of water in germinating castor beans as a function of time of imbibition (*a*) and as a function of the fractional increase in fresh mass (*b*).

apparent increase in T_1 with water content, when analysed as a single component, is rationalized as a relative increase with water content in the amount of the component with the shorter relaxation time.) Second, there is a smooth dependence of the T_1 values on water content. This gives us considerable confidence that the model does indeed reflect the real state of the water in the seeds, rather than being a mathematical subterfuge to better fit the data. This being the case, we can start to ask whether there is any other evidence supporting the two-component hypothesis and also what the two components might correspond to.

Dehydration studies

The relaxation times shown in figure 2 are suggestive of one water pool which is relatively 'free' and a second pool where the motion is more restricted, probably due to interaction with macromolecules. It might be expected that the latter pool would be harder to remove in dehydration experiments. To test this hypothesis, seeds which had taken up water for variable periods, were placed in a vacuum oven at 20 °C and left to reach a constant mass. The temperature was then increased and the process repeated. Results are shown in figure 3 for populations of seeds which had taken up water for (*a*) 10 h and (*b*) 90 h. In both cases there is a water fraction which resists removal at 20 °C but which comes off at 30 °C. The amount (absolute and relative) of this more tightly bound fraction is greater at the higher water content following 90 h of water uptake, in agreement with the two-component hypothesis.

PHILOSOPHICAL TRANSACTIONS OF THE ROYAL SOCIETY A MATHEMATICAL, PHYSICAL & ENGINEERING SCIENCES

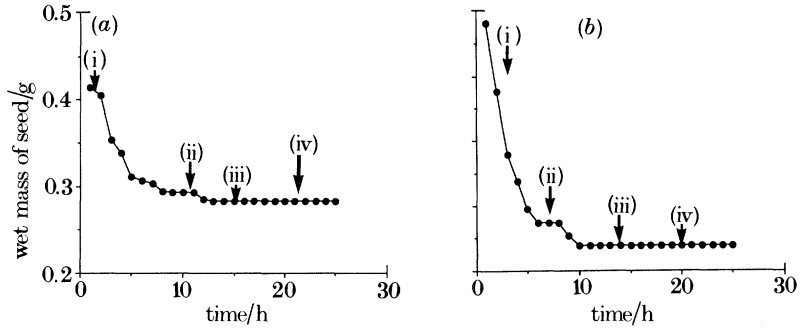

Figure 3. Dehydration of castor bean seed in a vacuum oven following (*a*) 10 h and (*b*) 90 h of imbibition. Temperature jumps are indicated by arrows, and are (i) 20 °C, (ii) 30 °C, (iii) 40 °C, (iv) 50 °C.

Fractionation experiments

The question naturally arises as to the nature of the two water pools. They could correspond to different anatomical regions within the developing seed, endosperm and embryo, for example, or the compartmentation could be microscopic: for example, the more tightly bound fraction could be the water associated with cell walls. Accordingly, seeds were dissected into endosperm and embryo. The T_1 values for water in the embryo are long (typically 1.7 s compared with values in the endosperm of about 0.3 s). However, it would be expected that the proportion of the embryo associated water should increase with total fresh mass, rather than *vice versa*. Interestingly, differences in the 'lipid' T_1 values were also observed between embryo and endosperm. The endosperm lipid T_1 value of 0.48 s reflects genuine storage lipid, whereas the higher embryonic value of approximately 1.7 s probably arises from smaller molecules derived from the breakdown of storage lipid and protein.

4. NMR microscopy

The read (frequency encoding) gradient in the three-dimensional Fourier imaging sequence was increased to ensure that pixels were separated by more than their natural linewidth. This, together with a lipid saturation pulse, greatly improved the clarity of the seed images. Figure 4 shows eight consecutive slices ((*a*) 18–21; (*b*) 22–25)) from a 32-slice data-set obtained from a seed after four days of water uptake. In slices 18 and 19 (upper left and right of (*a*), respectively), the cotyledons are clearly visible running through the centre of the endosperm. The primary root is visible in all slices; in cross-section in slices 18–22 and in increasingly oblique section in slices 23–25. The centrally located vascular tissue of the primary root is clearly visible in all sections. Secondary roots can be seen in cross section as 'bright' spots in all slices and also in longitudinal section in slices 22–25. The cotyledons can be seen merging to form the primary stem from slice 20. In slices 21 and 22 the branching of the primary stem into the left stalk is also visible, with the xylem tissue highlighted. As the radicle emerges from the base of the seed, discrete vascular bundles from, consisting of xylem phloem and cambium. The bundles can be seen in slices 24 and 25. Higher-resolution images (not shown) reveal the presence of eight discrete bundles in agreement with studies using optical microscopy on cut sections. The 'hazy shadows' evident, particularly in (*b*) arise from eddy current effects which are

PHILOSOPHICAL TRANSACTIONS OF THE ROYAL SOCIETY A MATHEMATICAL, PHYSICAL & ENGINEERING SCIENCES

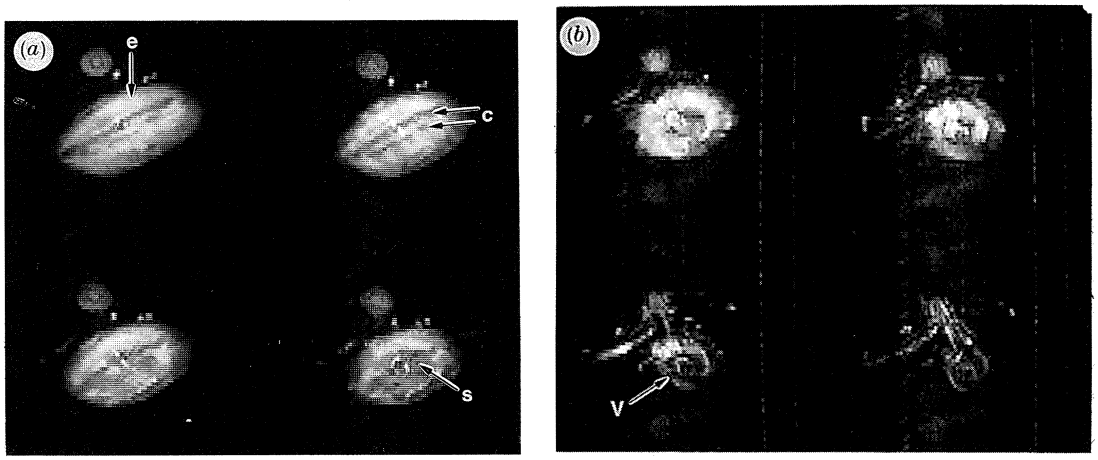

Figure 4. Slices (*a*) 18–21 and (*b*) 22–25 from a 32-slice data-set recorded from a developing castor bean seed after four days of water uptake. A T_R value of 1.0 s was used. The positions of the cotyledons (c), endosperm (e), leaf shoot (s) and vascular bundle (v) are indicated.

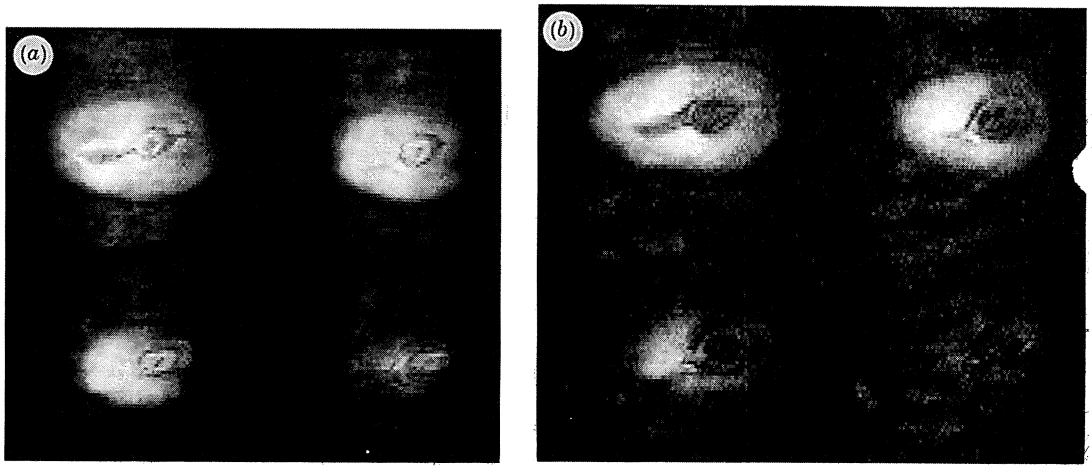

Figure 5. Slices 12–15 from 32-slice data-sets from a developing castor bean seed after four days of water uptake, recorded using an inversion null sequence with T_I set to (*a*) 1.37 s and (*b*) 0.34 s.

present in these images. The echo time was deliberately shortened to the point that theses effects were just evident to minimize the loss of signal from T_2 decay, a major problem in these very short T_2 systems.

These comparatively low-resolution images, recorded at a T_R of 1.0 s, reveal the anatomy of the developing seed well and allow structures to be followed right through the intact seed. However, they do not in themselves tell us very much about the state of the water giving rise to the signals. In an attempt to distinguish between the two major pools of water suggested by the relaxation time studies above, a parallel three-dimensional imaging experiment was performed in an interleaved fashion, with a T_R value of 0.3 s. This should have discriminated heavily against the more slowly relaxing component. However, the only noteworthy difference between the two sets of images was a generally decreased SNR in the more saturated (lower T_R) case.

PHILOSOPHICAL TRANSACTIONS OF THE ROYAL SOCIETY A MATHEMATICAL, PHYSICAL & ENGINEERING SCIENCES

Better discrimination on the basis of relaxation time differences was sought using the inversion null sequence. Two such experiments were performed in interleaved fashion on a four-day old seed. A comparison between four sections near the base of the seed is shown in figure 5. In (*a*), T_1 was 1.37 s, giving a null signal for the water pool with a long T_1 value, whereas in (*b*), T_1 was 0.34 s, giving a null for the short T_1 component. There are clearly regions with both long and short T_1 components within the endosperm. What is especially interesting is the preponderance of the short T_1 component within the vascular structure. *A priori*, it might have been thought that it would have been the longer T_1 component, corresponding to free water, which should be found in this region.

5. Conclusions

The T_1 water relaxation time measurements strongly suggest the presence of two primary pools of water in developing castor bean seeds. NMR microscopy reveals a wealth of anatomical detail in a completely non-invasive fashion but has not so far provided a unique assignment for these water pools. Inversion null images indicate that both free and the less mobile water fractions coexist at least within the endosperm. The compartmentation could therefore be microscopic in nature. The lack of any significant free water signal within the vascular tissue near the base of the developed seed is an interesting but not completely isolated observation. It merits further investigation.

The main limitation in the imaging studies reported was the echo times which are long relative to the water T_2 s. With the present gradient sets, the echo time cannot be further reduced without generating large eddy current artefacts. The use of shielded gradient systems would greatly ameliorate the situation (Mansfield & Chapman 1986).

References

Bewley, J. D. & Black, M. 1978 *Physiology and biochemistry of seeds in relation to germination*, vol. 1. *Development, germination and growth*. Berlin and Heidelberg: Springer-Verlag.

Edelstein, W. A., Hutchison, J. M. S., Johnson, G. & Redpath, T. 1980 Spin warp imaging and applications to whole body imaging. *Phys. med. Biol.* **25**, 751–756.

Frenkiel, T. A., Jasinski, A. & Morris, P. G. 1988 Apparatus for generation of magnetic field gradient waveforms for NMR imaging. *J. Phys.* E **21**, 374–377.

Mansfield, P. & Chapman, B. 1986 Active magnetic screening of gradient coils in NMR imaging. *J. magn. Reson.* **66**, 573–576.

Marriot, K. M. & Northcote, D. H. 1975*a* The breakdown of lipid in the endosperm of germinating castor beans. *Biochem. J.* **148**, 139–144.

Marriot, K. M. & Northcote, D. H. 1975*b* The induction of enzyme activity in the endosperm of germinating castor-bean seeds. *Biochem. J.* **152**, 65–70.

Martin, C. & Northcote, D. H. 1981 Qualitative and quantitative changes in mRNA of castor beans during the initial stages of germination. *Planta* **151**, 189–197.

Morris, P. G. 1986 *NMR imaging in medicine and biology*. Oxford University Press.

Morris, P. G., Jasinski, A. & McIntyre, D. J. O. 1990 NMR microscopy of plants. In *Modern microscopies: techniques and applications* (ed. P. J. Duke & A. G. Michette), pp. 171–183. New York: Plenum Press.

PHILOSOPHICAL TRANSACTIONS OF THE ROYAL SOCIETY A MATHEMATICAL, PHYSICAL & ENGINEERING SCIENCES

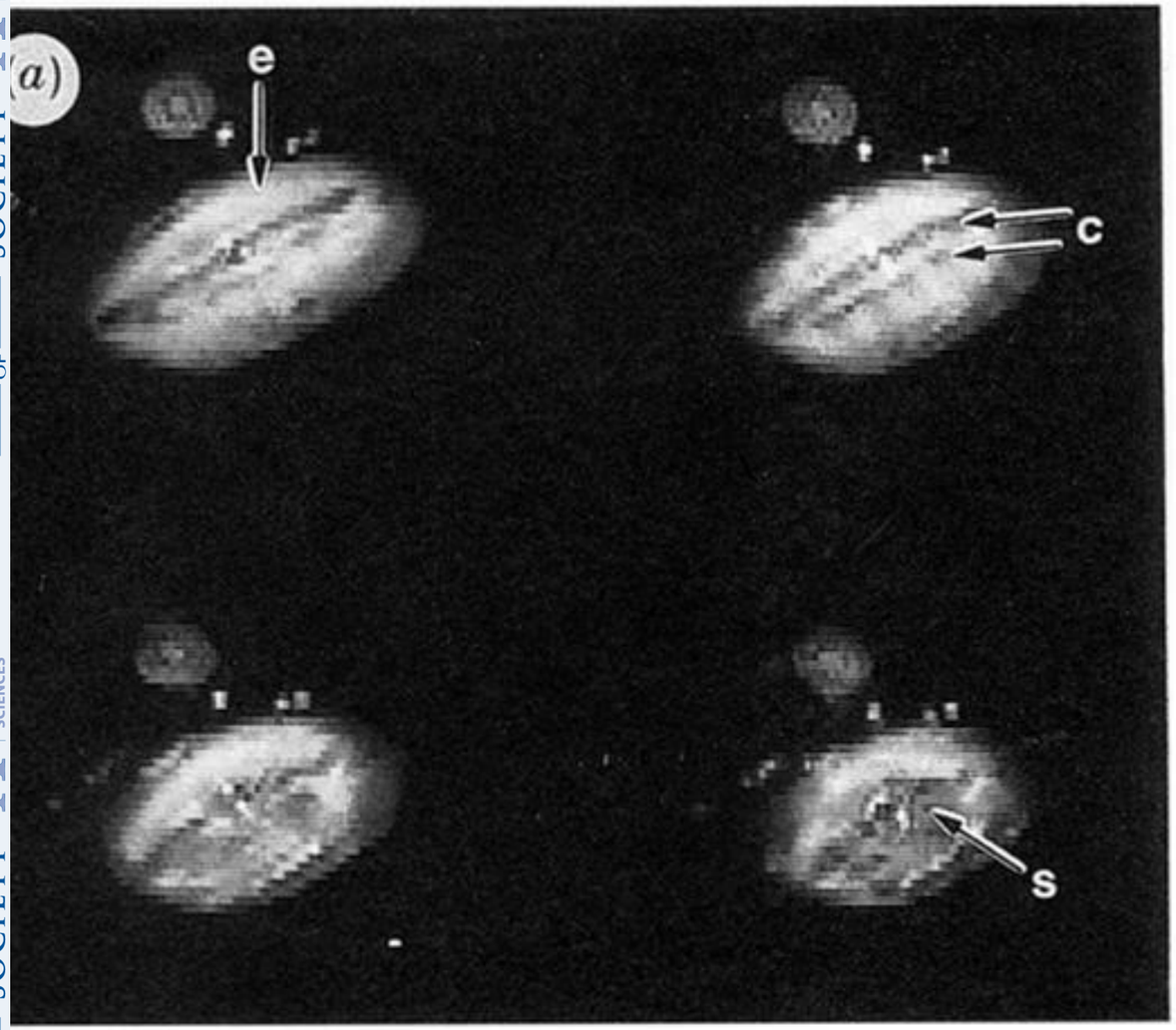

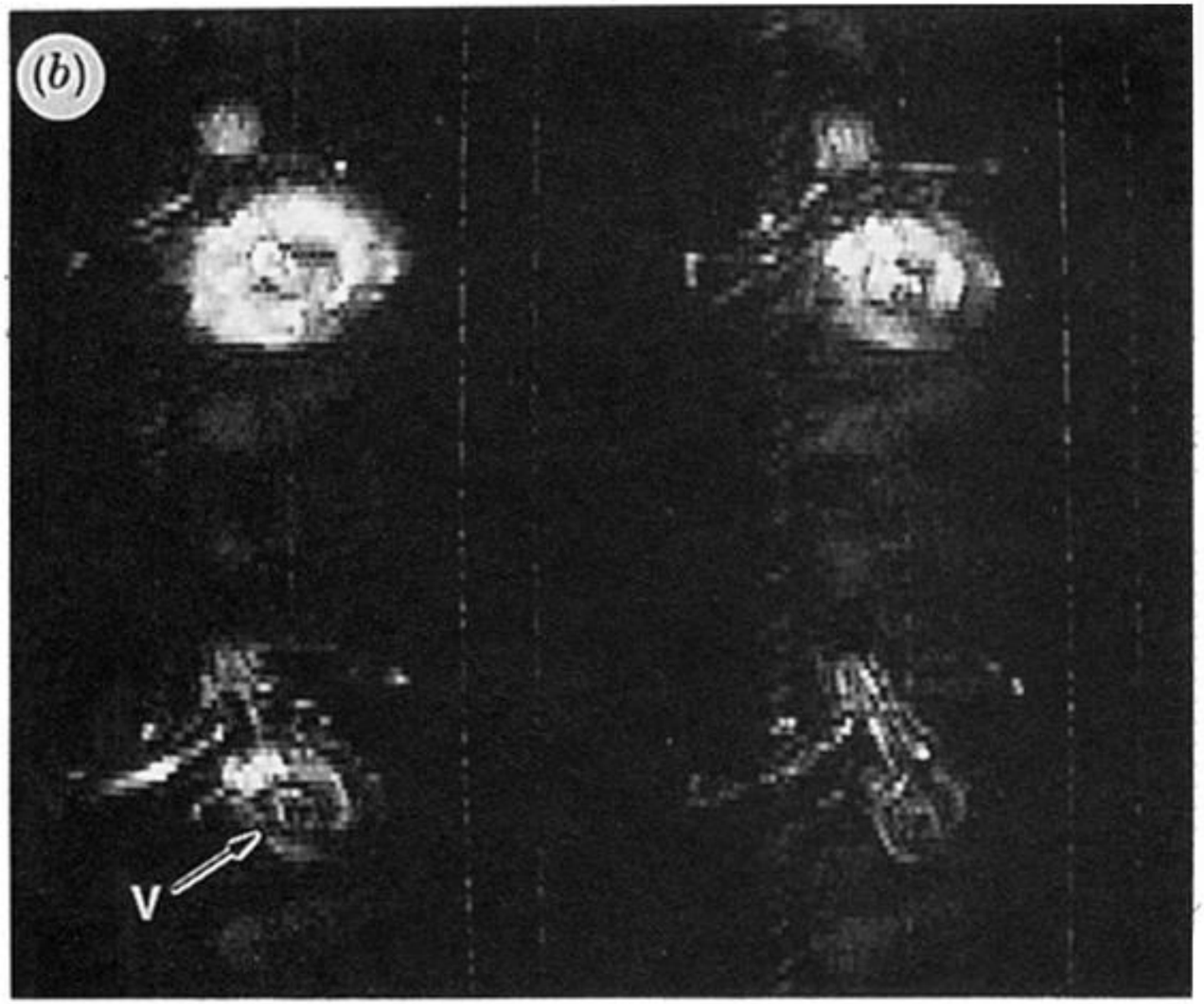

Figure 4. Slices (*a*) 18–21 and (*b*) 22–25 from a 32-slice data-set recorded from a developing castor bean seed after four days of water uptake. A T_R value of 1.0 s was used. The positions of the cotyledons (c), endosperm (e), leaf shoot (s) and vascular bundle (v) are indicated.

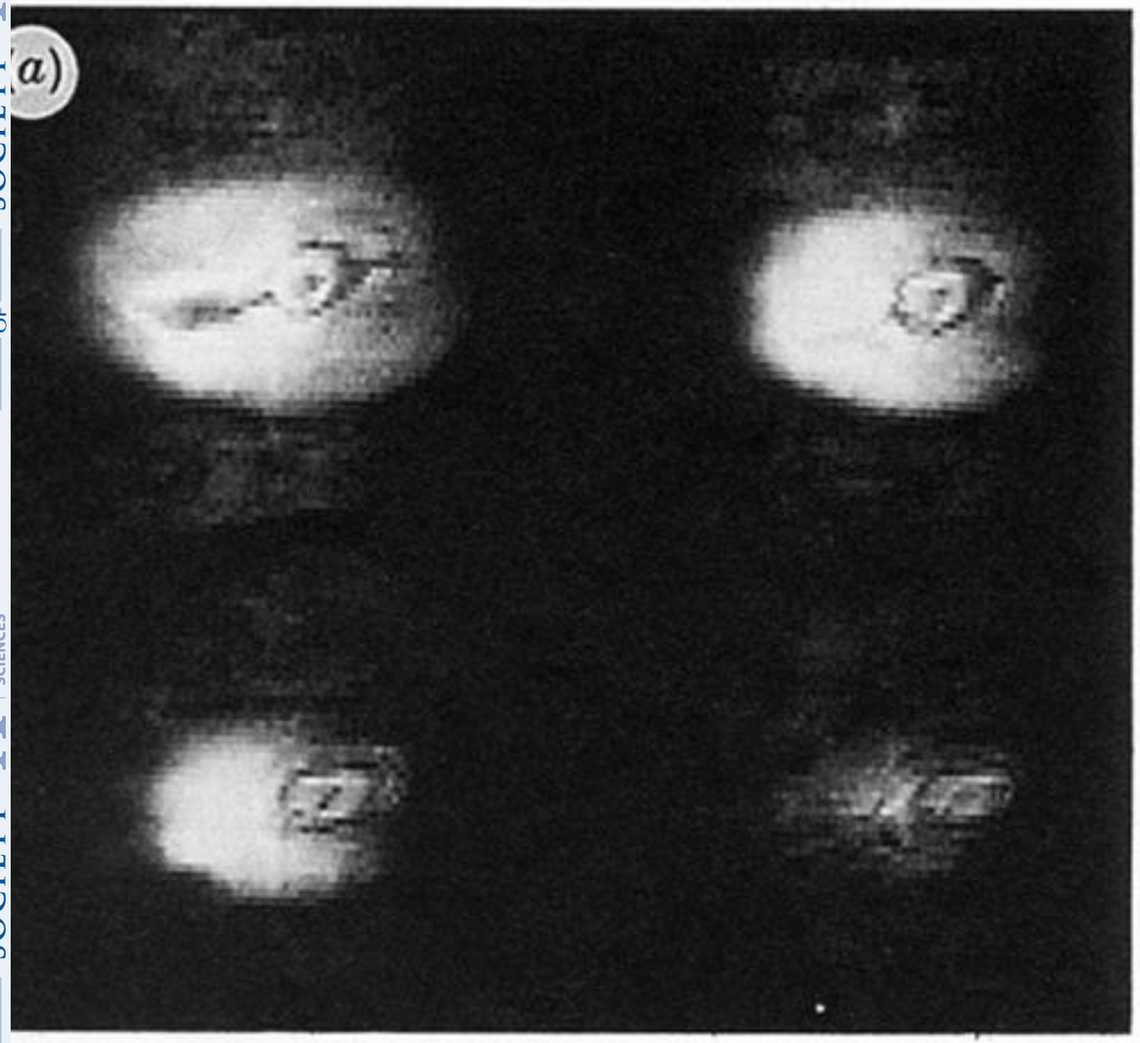

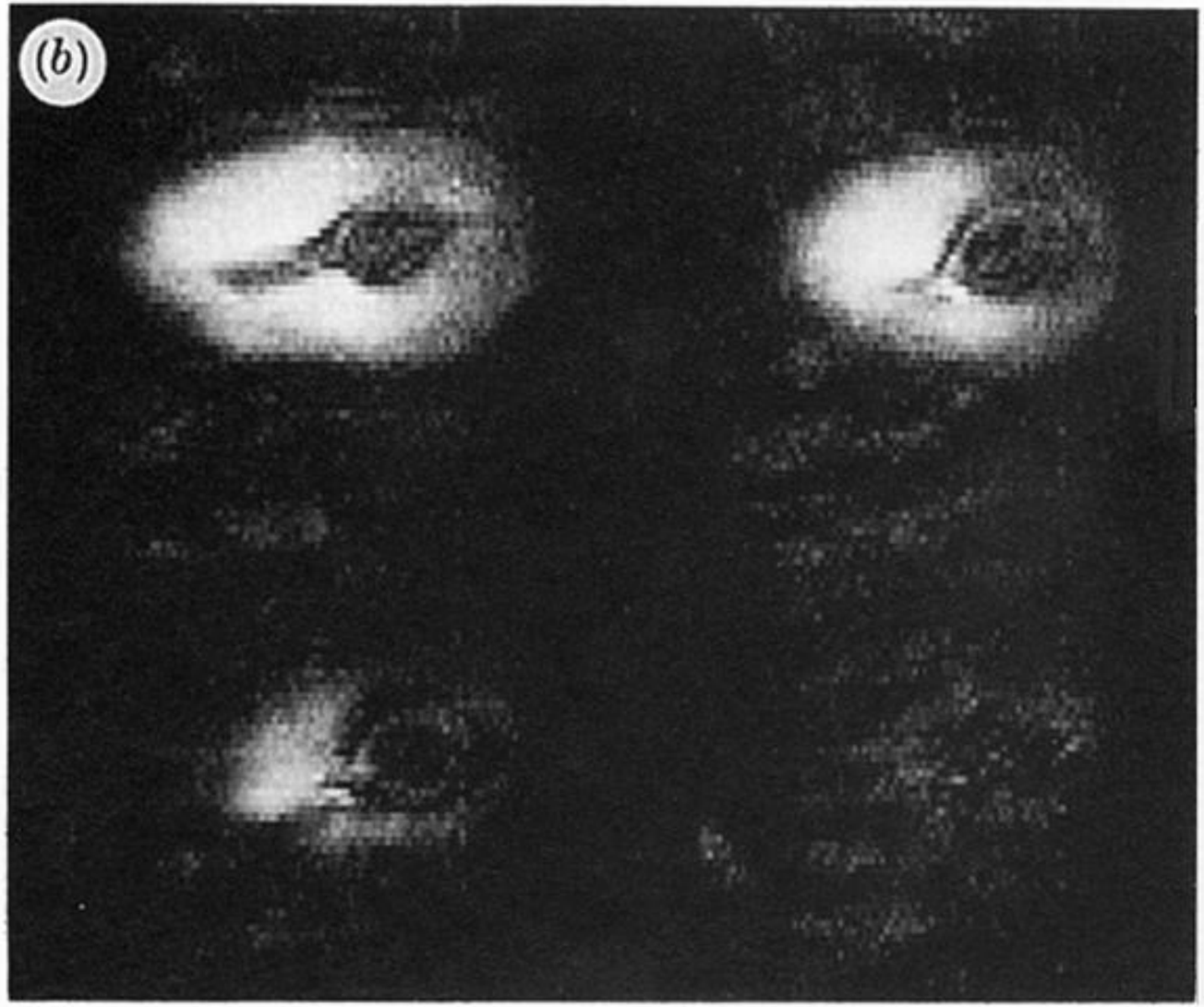

Figure 5. Slices 12–15 from 32-slice data-sets from a developing castor bean seed after four days of water uptake, recorded using an inversion null sequence with T_I set to (*a*) 1.37 s and (*b*) 0.34 s.